Differential Games Based Autonomous Rendezvous for Aerial Refueling

Ezra Tal and Tal Shima

Abstract An integrated guidance law and auto-pilot for autonomous rendezvous towards aerial refueling using the probe-and-drogue system is presented. For the derivation the rendezvous problem is considered as a differential game in which the trailing aircraft's objective is to capture the drogue. A linear quadratic cost formulation is utilized in order to develop an optimal control expression for pursuer aircraft elevator, ailerons, and rudder control, as well as optimal evasive action. Optimal evasive action herein represents the worst-case drogue movement. Results of numerical simulations using a longitudinal lateral-directional flight dynamic model of a realistic aircraft are presented.

1 Introduction

Rendezvous for aerial refueling refers to the connecting of the probe on the receiver aircraft, and the drogue at the end of the hose on the tanker aircraft, before commencement of the actual refueling. For a successful rendezvous both position and velocity must be equal, which is complicated by the movement of the drogue. Due to aerodynamic coupling between tanker aircraft, drogue, and receiver aircraft the rendezvous is one of the most challenging maneuvers to perform for pilots.

The emergence of autonomous unmanned aerial vehicles calls for the development of guidance and control laws that enable autonomous exe-

Ezra Tal
Delft University of Technology, Faculty of Aerospace Engineering, Delft, 2629 HS, Netherlands e-mail: e.a.tal@student.tudelft.nl

Tal Shima
Technion - Israel Institute of Technology, Faculty of Aerospace Engineering, Haifa, 32000, Israel e-mail: tal.shima@technion.ac.il

cution of the rendezvous for aerial refueling. The problem has been approached using various methods for robust and adaptive controller design [Wang et al.(2008), Pachter et al.(1997)], and incorporating sensor systems [Tandale et al.(2006)].

Owing to similarities to the problem of missile guidance, control methods based on the concepts of proportional navigation and line of sight angle control have been proposed [Ochi and Kominami(2005)]. Also originating from missile guidance is the concept of zero-sum pursuit-evasion differential game-based guidance laws [Bryson and Ho(1969)]. The method presented in this paper is based on the formulation of the rendezvous for aerial refueling as such a zero-sum pursuit-evasion differential game. Within this formulation the drogue acts as evader and the recipient aircraft as pursuer. The cost of the zero-sum game consists of the final position and velocity differences between drogue and recipient aircraft. It has been shown that for the case of unpredictable evasive action differential game guidance laws surpass optimal control based guidance laws in terms of performance [Anderson(1981)].

In order to account for control boundaries, weighed quadratic terms are added to the cost function. These terms act as penalty functions on the otherwise unbounded control inputs of both pursuer and evader, leading to a linear quadratic (LQ) differential game formulation [Bryson and Ho(1969)].

Within the zero-sum differential game it is the objective of the pursuer to minimize the cost, whereas it is the aim of the evader to maximize this cost. The solution of the game consists of optimal control actions for both pursuer and evader. The former serves as the autonomous aerial refueling guidance law, while the latter can be considered a worst-case movement of the drogue. Hence, the optimal evasive action can be used to give a measure of the robustness of the guidance law with respect to any possible movement by the drogue.

The recipient aircraft is represented by a model involving both dynamic and kinematic states leading to the derivation of an integrated guidance law and autopilot. In previous work the development of an integrated controller for missile autopilot guidance motivated by a differential game formulation has been presented [Shima et al.(2006)]. Application to elevator control for autonomous rendezvous using a longitudinal flight dynamic model has been shown as well [Tal and Shima(2015)].

In the current work, the integrated controller commands elevator, ailerons, and rudder. The concept of a differential games multi-control guidance law has been presented in the context of a dual-control guidance law for interception using missiles with multiple control surfaces [Shima and Golan(2007)].

2 Dynamics Modeling

A linearized rendezvous model considering movement perpendicular to the fixed relative horizontal closing speed V_c with which the recipient aircraft is approaching the drogue is used. The fixed relative horizontal closing speed leads to a known time of interception t_f. An overview of the rendezvous geometry is given in Figure 1.

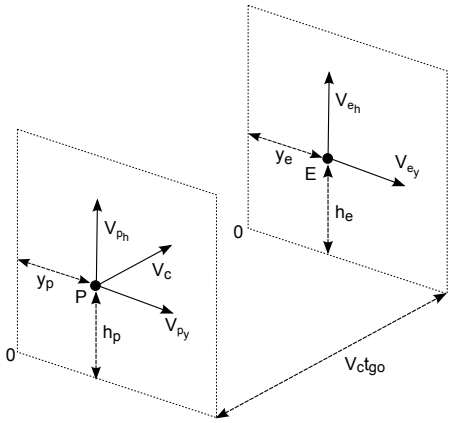

Fig. 1 Rendezvous geometry

The drogue, i.e. evader, has direct control of its acceleration in both the horizontal and vertical plane. The position is given by double integration of the corresponding acceleration input. For vertical position

$$\ddot{h}_e = a_e^{max} v_1 \tag{1}$$

and equivalently for lateral position

$$\ddot{y}_e = a_e^{max} v_2 \tag{2}$$

where a_e^{max} is the maximum magnitude of acceleration per direction, which is set equal for both directions, with $a_e^{max} > 0$, and v_1 and v_2 are normalized control variables with $|v_i| \leq 1$ for $i \in \{1, 2\}$.

By introducing the vertical evader speed V_{e_h} and the lateral evader speed V_{e_y}, the evader kinematics can be formulated as a system of first order differential equations

$$\begin{cases} \dot{h}_e = V_{e_h} \\ \dot{y}_e = V_{e_y} \\ \dot{V}_{e_h} = a_e^{max} v_1 \\ \dot{V}_{e_y} = a_e^{max} v_2 \end{cases} \tag{3}$$

The aircraft, i.e. pursuer, kinematic and dynamic equations are linearized around a horizontal symmetric steady flight condition. The state variables correspond to the state's deviation from this trim condition.

The aircraft vertical position is given by integration of its vertical speed

$$\dot{h}_p = V_{p_h} = V_0(\theta - \alpha) \tag{4}$$

where V_0 is the total airspeed in trimmed condition, θ is the pitch angle, and α is the angle of attack. Assuming that V_0 is constant, the vertical acceleration is

$$\dot{V}_{p_h} = V_0(\dot{\theta} - \dot{\alpha}) = V_0(q - \dot{\alpha}) \tag{5}$$

where q is the pitch rate. The lateral speed is given by

$$\dot{y}_p = V_{p_y} = V_0(\psi + \beta - \alpha_0\phi) \tag{6}$$

where α_0 and θ_0 correspond to the trimmed angle of attack and pitch angle, respectively. The sideslip, heading, and roll angles are indicated by β, ψ, and ϕ, respectively. The lateral acceleration is then given by

$$\dot{V}_{p_y} = V_0(\dot{\psi} + \dot{\beta} - \alpha_0\dot{\phi}) = V_0(r + \dot{\beta} - \alpha_0\dot{\phi}) \tag{7}$$

where r is the yaw rate.

The force and moment contributions of $\dot{\alpha}$ and $\dot{\beta}$ are neglected. It is assumed that the aircraft and flight condition are perfectly symmetrical and that there is no longitudinal lateral-directional coupling due to engine rotor angular momentum. Consequently the linear system of kinematic and dynamic equations is uncoupled. The differential equations for the aircraft dynamics are formulated using dimensional stability and control derivatives. For the control surface dynamics first order lags with time constant τ_δ are assumed. The resulting system of first order equations is given by

$$\begin{cases} \dot{h}_p = V_{p_h} \\ \dot{y}_p = V_{p_y} \\ \dot{V}_{p_h} = -Z_\alpha\alpha - Z_q q - Z_{\delta_{ele}}\delta_{ele} \\ \dot{V}_{p_y} = g\phi + Y_\beta\beta + (Y_p - V_0\alpha_0)p + Y_r r + Y_{\delta_{ail}}\delta_{ail} + Y_{\delta_{rud}}\delta_{rud} \\ \dot{\phi} = p + \theta_0 r \\ V_0\dot{\alpha} = Z_\alpha\alpha + (V_0 + Z_q)q + Z_{\delta_{ele}}\delta_{ele} \\ V_0\dot{\beta} = g\phi + Y_\beta\beta + Y_p p + (Y_r - V_0)r + Y_{\delta_{ail}}\delta_{ail} + Y_{\delta_{rud}}\delta_{rud} \\ \dot{p} = L_\beta\beta + L_p p + L_r r + L_{\delta_{ail}}\delta_{ail} + L_{\delta_{rud}}\delta_{rud} \\ \dot{q} = M_\alpha\alpha + M_q q + M_{\delta_{ele}}\delta_{ele} \\ \dot{r} = N_\beta\beta + N_p p + N_r r + N_{\delta_{ail}}\delta_{ail} + N_{\delta_{rud}}\delta_{rud} \\ \dot{\delta}_{ele} = -\frac{1}{\tau_\delta}\delta_{ele} + \frac{1}{\tau_\delta}\delta_{ele}^{max}u_1 \\ \dot{\delta}_{ail} = -\frac{1}{\tau_\delta}\delta_{ail} + \frac{1}{\tau_\delta}\delta_{ail}^{max}u_2 \\ \dot{\delta}_{rud} = -\frac{1}{\tau_\delta}\delta_{rud} + \frac{1}{\tau_\delta}\delta_{rud}^{max}u_3 \end{cases} \tag{8}$$

where p is the roll rate, and δ_{ele}^{max}, δ_{ail}^{max}, and δ_{rud}^{max} are the maximum elevator, aileron, and rudder deflection magnitudes, respectively. The inputs u_1, u_2, and u_3 are normalized control variables with $|u_i| \leq 1$ for $i \in \{1, 2, 3\}$.

Several observations can be made regarding the resulting system of differential equations. The model is considerably more complicated than the idealized missile dynamics models that are often used for the application of differential game-based guidance [Shinar and Shima(2012)], as it is composed of both dynamical and kinematical states leading to an integrated guidance law and autopilot design. The system is not fully controllable by $\mathbf{u}$, as is typical for linear aircraft models involving both longitudinal and lateral-directional dynamic and kinematic states.

An interesting feature is the fact that the aircraft vertical speed is non-minimum phase with regard to elevator control: The additional lift of a positive elevator deflection will initially result in a positive vertical acceleration, after which it leads to pitch down and negative vertical acceleration. Similar non-minimum phase behavior is exhibited by the response of the lateral speed to aileron and rudder inputs, due to the direct side-force and subsequent respective roll and yaw rates that these inputs cause. These phenomena are relevant, as they lead to control reversal during the final part of rendezvous.

A state-space system incorporating both the receiver aircraft (pursuer) and drogue (evader) dynamics can now be defined. Since the aircraft model is already formulated including vertical and lateral positions and speeds as states, the composite system can straightforwardly be formulated as

$$\dot{\mathbf{x}} = \mathbf{A}\mathbf{x} + \mathbf{B}\mathbf{u} + \mathbf{C}\mathbf{v} \tag{9}$$

where

$$\mathbf{x} = \begin{bmatrix} h_p - h_e \\ y_p - y_e \\ V_{p_h} - V_{e_h} \\ V_{p_y} - V_{e_y} \\ \phi \\ \alpha \\ \beta \\ p \\ q \\ r \\ \delta_{ele} \\ \delta_{ail} \\ \delta_{rud} \end{bmatrix}, \tag{10}$$

$$\mathbf{A} = \begin{bmatrix} \mathbf{0}_{2\times2} & \mathbf{I}_{2\times2} & & & \mathbf{0}_{2\times6} & & & & \mathbf{0}_{2\times3} & \\ & & 0 & -Z_\alpha & 0 & 0 & -Z_q & 0 & -Z_{\delta_{ele}} & 0 & 0 \\ & & g & 0 & Y_\beta & Y_p - V_0\alpha_0 & 0 & Y_r & 0 & Y_{\delta_{ail}} & Y_{\delta_{rud}} \\ & & 0 & 0 & 0 & 1 & 0 & \theta_0 & 0 & 0 & 0 \\ & & 0 & \frac{Z_\alpha}{V_0} & 0 & 0 & 1+\frac{Z_q}{V_0} & 0 & \frac{Z_{\delta_{ele}}}{V_0} & 0 & 0 \\ \mathbf{0}_{8\times2} & \mathbf{0}_{8\times2} & \frac{g}{V_0} & 0 & \frac{Y_\beta}{V_0} & \frac{Y_p}{V_0} & 0 & \frac{Y_r}{V_0}-1 & 0 & \frac{Y_{\delta_{ail}}}{V_0} & \frac{Y_{\delta_{rud}}}{V_0} \\ & & 0 & 0 & L_\beta & L_p & 0 & L_r & 0 & L_{\delta_{ail}} & L_{\delta_{rud}} \\ & & 0 & M_\alpha & 0 & 0 & M_q & 0 & M_{\delta_{ele}} & 0 & 0 \\ & & 0 & 0 & N_\beta & N_p & 0 & N_r & 0 & N_{\delta_{ail}} & N_{\delta_{rud}} \\ \mathbf{0}_{3\times2} & \mathbf{0}_{3\times2} & & & & \mathbf{0}_{3\times6} & & & & -\frac{1}{\tau_\delta}\mathbf{I}_{3\times3} & \end{bmatrix}, \tag{11}$$

$$\mathbf{B} = \begin{bmatrix} & \mathbf{0}_{10\times3} & \\ \frac{\delta_{ele}^{max}}{\tau_\delta} & 0 & 0 \\ 0 & \frac{\delta_{ail}^{max}}{\tau_\delta} & 0 \\ 0 & 0 & \frac{\delta_{rud}^{max}}{\tau_\delta} \end{bmatrix}, \ \mathbf{C} = \begin{bmatrix} \mathbf{0}_{2\times2} \\ -a_e^{max}\mathbf{I}_{2\times2} \\ \mathbf{0}_{9\times2} \end{bmatrix} \tag{12}$$

For a successful rendezvous the first four states, vertical and lateral position and speed difference, must be nulled. Hence the pursuer is minimizing these values, whereas the evader is maximizing these values. Both are assumed to have perfect knowledge of the entire state.

The admissible gamespace is limited by several constraints. The states ϕ, α, β, p, q, and r are limited by operational limits during the rendezvous. The aircraft control surface states are limited by their respective maximum deflection magnitudes.

3 Guidance Law

Three elements are taken into account in the formulation of the linear-quadratic cost function that is used for guidance law optimization: Terminal relative position and relative speed contributions, the cost of pursuer control, and the cost of evader control. The relative position R is the Euclidean distance between the evader and the pursuer in the vertical-lateral plane and the relative speed V_r is the Euclidean norm of the difference between their velocities in the aforementioned plane. The cost function is given by

$$J = \frac{1}{2}R^2(t_f) + \frac{Q_V}{2}{V_r}^2(t_f) + \frac{1}{2}\int_{t_0}^{t_f} \left(\alpha_1 {u_1}^2(t) + \alpha_2 {u_2}^2(t) + \alpha_3 {u_3}^2(t) - \beta_1 {v_1}^2(t) - \beta_2 {v_2}^2(t)\right) \mathrm{d}t \tag{13}$$

where Q_V, α_1, α_2, α_3, β_1, and β_2 are all non-negative weights. Note that if the weights approach zero an interception guidance law is found. Equivalently, setting $Q_V \to \infty$ leads to a nulling of relative speed.

3.1 Order Reduction

In order to reduce the order of the problem the terminal cost $\mathbf{Z}(t_f)$ is introduced. In order to express the terminal cost the zero-effort vector is used. Making use of the terminal projection transformation [Bryson and Ho(1969)] the zero-effort vector is defined as

$$\mathbf{Z}(t) = \mathbf{D}\mathbf{\Phi}(t_f, t)\mathbf{x}(t) \tag{14}$$

where

$$\mathbf{D} = \begin{bmatrix} \mathbf{I}_{4\times 4} & \mathbf{0}_{9\times 4} \end{bmatrix} \tag{15}$$

and $\mathbf{\Phi}(t_f, t)$ is the transition matrix associated with Eq. (9)

$$\mathbf{\Phi}(t_f, t) = e^{\mathbf{A}t_{go}} \tag{16}$$

with

$$t_{go} = t_f - t \tag{17}$$

Given the time-derivative of the transition matrix

$$\dot{\mathbf{\Phi}}(t_f, t) = -\mathbf{\Phi}(t_f, t)\mathbf{A} \tag{18}$$

the time-derivative of the zero-effort vector is

$$\dot{\mathbf{Z}}(t) = \tilde{\mathbf{B}}(t_f, t)\mathbf{u}(t) + \tilde{\mathbf{C}}(t_f, t)\mathbf{v}(t) \tag{19}$$

where

$$\tilde{\mathbf{B}}(t_f, t) = \mathbf{D}\mathbf{\Phi}(t_f, t)\mathbf{B},\ \tilde{\mathbf{C}}(t_f, t) = \mathbf{D}\mathbf{\Phi}(t_f, t)\mathbf{C} \tag{20}$$

The zero-effort vector includes contributions of both the vertical and lateral position and speed differences. It represents the vertical and lateral position and speed differences that would be created by the time t_f if none of the parties were to apply any control from time t onward. $Z_1(t)$ is referred to as the vertical zero-effort miss distance (VZEM), $Z_2(t)$ is referred to as the lateral zero-effort miss distance (LZEM), $Z_3(t)$ is referred to as the vertical zero-effort speed difference (VZES), and $Z_4(t)$ is referred to as the lateral zero-effort speed difference (LZES). The zero-effort vector at t_f is given by

$$\mathbf{Z}(t_f) = \mathbf{D}\mathbf{x}(t_f) = \begin{bmatrix} x_1(t_f) \\ x_2(t_f) \\ x_3(t_f) \\ x_4(t_f) \end{bmatrix} \tag{21}$$

Using the zero-effort vector and the definition of the Euclidean norm the LQ cost function J can now be reformulated as

$$J = \frac{1}{2}\mathbf{Z}^T(t_f)\mathbf{Q}\mathbf{Z}(t_f) + \frac{1}{2}\int_{t_0}^{t_f} \left(\mathbf{u}^T(t)\boldsymbol{\alpha}\mathbf{u}(t) - \mathbf{v}^T(t)\boldsymbol{\beta}\mathbf{v}(t)\right) \mathrm{d}t \tag{22}$$

where

$$\mathbf{Q} = \begin{bmatrix} \mathbf{I}_{2\times 2} & \mathbf{0}_{2\times 2} \\ \mathbf{0}_{2\times 2} & Q_V\mathbf{I}_{2\times 2} \end{bmatrix},\ \boldsymbol{\alpha} = \begin{bmatrix} \alpha_1 & 0 & 0 \\ 0 & \alpha_2 & 0 \\ 0 & 0 & \alpha_3 \end{bmatrix},\ \boldsymbol{\beta} = \begin{bmatrix} \beta_1 & 0 \\ 0 & \beta_2 \end{bmatrix} \tag{23}$$

It should be noted that no explicit constraints are defined; the conditions $|u_i(t)| \leq 1\ \forall t$ for $i \in \{1,2,3\}$ and $|v_i(t)| \leq 1\ \forall t$ for $i \in \{1,2\}$ as well as the operational constraints on ϕ, α, β, p, q, and r are to be satisfied by appropriate selection of $\mathbf{Q}$, $\boldsymbol{\alpha}$ and $\boldsymbol{\beta}$.

3.2 Optimal Control

Using the reduced-order LQ cost function the differential game can now be solved. The Hamiltonian is given by (time indices are omitted for brevity)

$$H = L + \boldsymbol{\lambda}_{\mathbf{Z}}^T\mathbf{f} \tag{24}$$

where

$$L = \frac{1}{2}\left(\mathbf{u}^T(t)\boldsymbol{\alpha}\mathbf{u}(t) - \mathbf{v}^T(t)\boldsymbol{\beta}\mathbf{v}(t)\right),\ \mathbf{f} = \dot{\mathbf{Z}} = \tilde{\mathbf{B}}\mathbf{u} + \tilde{\mathbf{C}}\mathbf{v} \tag{25}$$

The adjoint equation is then given by

$$\dot{\boldsymbol{\lambda}}_{\mathbf{Z}}^T = -\left(\frac{\partial L}{\partial \mathbf{Z}} + \boldsymbol{\lambda}_{\mathbf{Z}}^T\frac{\partial \mathbf{f}}{\partial \mathbf{Z}}\right) = -\left(\mathbf{0}_{1\times 4} + \boldsymbol{\lambda}_{\mathbf{Z}}^T\mathbf{0}_{4\times 4}\right) = \mathbf{0}_{1\times 4} \tag{26}$$

and

$$\boldsymbol{\lambda}_{\mathbf{Z}}^T(t_f) = \frac{\partial\left(\frac{1}{2}\mathbf{Z}^T(t_f)\mathbf{Q}\mathbf{Z}(t_f)\right)}{\partial \mathbf{Z}} = \mathbf{Z}^T(t_f)\mathbf{Q} \tag{27}$$

which results in

$$\boldsymbol{\lambda}_{\mathbf{Z}}(t) = \mathbf{Q}\mathbf{Z}(t_f) \tag{28}$$

In order to find the optimal control law the derivative of the Hamiltonian with regard to the control input is set to zero

$$\frac{\partial H}{\partial \mathbf{u}} = \mathbf{u}^T \boldsymbol{\alpha} + \mathbf{Z}^T(t_f)\mathbf{Q}\tilde{\mathbf{B}} = 0 \tag{29}$$

This results in the optimal pursuer control

$$\mathbf{u}^* = -\boldsymbol{\alpha}^{-1}\tilde{\mathbf{B}}^T\mathbf{Q}\mathbf{Z}(t_f) \tag{30}$$

Similarly it can be shown that the optimal evader control is

$$\mathbf{v}^* = \boldsymbol{\beta}^{-1}\tilde{\mathbf{C}}^T\mathbf{Q}\mathbf{Z}(t_f) \tag{31}$$

Integration after the substitution of the expressions for the optimal control actions into Eq. (19) gives

$$\mathbf{Z}(t_f) = \mathbf{Z}(t) + \mathbf{F}_{\boldsymbol{\alpha\beta}}(t_f, t)\mathbf{Z}(t_f) \tag{32}$$

where

$$\mathbf{F}_{\boldsymbol{\alpha\beta}}(t_f, t) = \int_t^{t_f} -\tilde{\mathbf{B}}(t_f, \xi)\boldsymbol{\alpha}^{-1}\tilde{\mathbf{B}}^T(t_f, \xi)\mathbf{Q} + \tilde{\mathbf{C}}(t_f, \xi)\boldsymbol{\beta}^{-1}\tilde{\mathbf{C}}^T(t_f, \xi)\mathbf{Q}\mathrm{d}\xi \tag{33}$$

Now the control laws can be written as functions of the current zero-effort vector as

$$\mathbf{u}^*(t) = -\boldsymbol{\alpha}^{-1}\tilde{\mathbf{B}}^T(t_f, t)\mathbf{Q}\left(\mathbf{I}_{4\times 4} - \mathbf{F}_{\boldsymbol{\alpha\beta}}(t_f, t)\right)^{-1}\mathbf{Z}(t) \tag{34}$$

$$\mathbf{v}^*(t) = \boldsymbol{\beta}^{-1}\tilde{\mathbf{C}}^T(t_f, t)\mathbf{Q}\left(\mathbf{I}_{4\times 4} - \mathbf{F}_{\boldsymbol{\alpha\beta}}(t_f, t)\right)^{-1}\mathbf{Z}(t) \tag{35}$$

3.3 Conjugate Point Analysis

Eq. (34) and Eq. (35) signify that a conjugate point exists if the matrix $(\mathbf{I} - \mathbf{F}_{\boldsymbol{\alpha\beta}}(t_f, t))$ is singular. In this case the trajectory may not be optimal going back in time beyond the conjugate point.

Considering that $\mathbf{F}_{\boldsymbol{\alpha\beta}} \to \mathbf{0}$ as $t_{go} \to 0$, $(\mathbf{I} - \mathbf{F}_{\boldsymbol{\alpha\beta}}(t_f, t)) \to \mathbf{I}$ and consequently $\Delta \to 1$, where $\Delta = \det(\mathbf{I} - \mathbf{F}_{\boldsymbol{\alpha\beta}}(t_f, t))$. Since $\mathbf{F}_{\boldsymbol{\alpha\beta}}$ is a continuous function of t, the optimal LQ differential game solution exists if

$$\Delta = \det(\mathbf{I} - \mathbf{F}_{\boldsymbol{\alpha\beta}}(t_f, t)) > 0 \quad \forall t \tag{36}$$

or equivalently using the analytic expression of the determinant

$$\Delta = \left(\kappa_1 + \kappa_2 - \kappa_1\kappa_2 + \kappa_3\kappa_4 - 1\right)\left(\kappa_5 + \kappa_6 - \kappa_5\kappa_6 + \kappa_7\kappa_8 - 1\right) > 0 \quad \forall t \tag{37}$$

where

$$\kappa_1 = \int_t^{t_f} \frac{a_e^{max2}}{\beta_1} {\phi_{1,3}}^2(t_f,\xi) - \frac{\delta_{ele}^{max2}}{\alpha_1 {\tau_\delta}^2} {\phi_{1,11}}^2(t_f,\xi)\mathrm{d}\xi \tag{38}$$

$$\kappa_2 = \int_t^{t_f} \frac{Q_V a_e^{max2}}{\beta_1} {\phi_{3,3}}^2(t_f,\xi) - \frac{Q_V \delta_{ele}^{max2}}{\alpha_1 {\tau_\delta}^2} {\phi_{3,11}}^2(t_f,\xi)\mathrm{d}\xi \tag{39}$$

$$\kappa_3 = \int_t^{t_f} \frac{Q_V a_e^{max2}}{\beta_1} \phi_{3,3}(t_f,\xi)\phi_{1,3}(t_f,\xi) - \frac{Q_V \delta_{ele}^{max2}}{\alpha_1 {\tau_\delta}^2} \phi_{3,11}(t_f,\xi)\phi_{1,11}(t_f,\xi)\mathrm{d}\xi \tag{40}$$

$$\kappa_4 = \int_t^{t_f} \frac{a_e^{max2}}{\beta_1} \phi_{3,3}(t_f,\xi)\phi_{1,3}(t_f,\xi) - \frac{\delta_{ele}^{max2}}{\alpha_1 {\tau_\delta}^2} \phi_{3,11}(t_f,\xi)\phi_{1,11}(t_f,\xi)\mathrm{d}\xi \tag{41}$$

$$\kappa_5 = \int_t^{t_f} \frac{a_e^{max2}}{\beta_2} {\phi_{2,4}}^2(t_f,\xi) - \frac{\delta_{ail}^{max2}}{\alpha_2 {\tau_\delta}^2} {\phi_{2,12}}^2(t_f,\xi) - \frac{\delta_{rud}^{max2}}{\alpha_3 {\tau_\delta}^2} {\phi_{2,13}}^2(t_f,\xi)\mathrm{d}\xi \tag{42}$$

$$\kappa_6 = \int_t^{t_f} \frac{Q_V a_e^{max2}}{\beta_2} {\phi_{4,4}}^2(t_f,\xi) - \frac{Q_V \delta_{ail}^{max2}}{\alpha_2 {\tau_\delta}^2} {\phi_{4,12}}^2(t_f,\xi) - \frac{Q_V \delta_{rud}^{max2}}{\alpha_3 {\tau_\delta}^2} {\phi_{4,13}}^2(t_f,\xi)\mathrm{d}\xi \tag{43}$$

$$\kappa_7 = \int_t^{t_f} \frac{Q_V a_e^{max2}}{\beta_2} \phi_{2,4}(t_f,\xi)\phi_{4,4}(t_f,\xi) - \frac{Q_V \delta_{ail}^{max2}}{\alpha_2 {\tau_\delta}^2} \phi_{2,12}(t_f,\xi)\phi_{4,12}(t_f,\xi) - \frac{Q_V \delta_{rud}^{max2}}{\alpha_3 {\tau_\delta}^2} \phi_{2,13}(t_f,\xi)\phi_{4,13}(t_f,\xi)\mathrm{d}\xi \tag{44}$$

$$\kappa_8 = \int_t^{t_f} \frac{a_e^{max2}}{\beta_2} \phi_{2,4}(t_f,\xi)\phi_{4,4}(t_f,\xi) - \frac{\delta_{ail}^{max2}}{\alpha_2 {\tau_\delta}^2} \phi_{2,12}(t_f,\xi)\phi_{4,12}(t_f,\xi) - \frac{\delta_{rud}^{max2}}{\alpha_3 {\tau_\delta}^2} \phi_{2,13}(t_f,\xi)\phi_{4,13}(t_f,\xi)\mathrm{d}\xi \tag{45}$$

with $\phi_{i,j}(t_f,t)$ the element on the i-th row of the j-th column of $\mathbf{\Phi}(t_f,t)$. An analytic expression for $\mathbf{\Phi}(t_f,t)$ can be found by performing an inverse Laplace transform of $(s\mathbf{I}-\mathbf{A})^{-1}$, but is too lengthy to be shown here.

Examination of Eq. (37) - Eq. (45) shows that $\Delta \to 1\ \forall t$ as $\mu \to \infty$, where $\mu = \alpha_1 = \alpha_2 = \beta_1 = \beta_2 = \beta_3$. The maximum value of Δ on the closed interval $\{t_{go} \in \mathbf{R} | 0 \leq t_{go} \leq 10\}$ was calculated as a function of μ in order to assess the existence of an LQ differential game solution on the aforementioned interval for the case with $Q_V = 0.5$, and $a_e^{max} = 2$ ft/s^2 using parameters corresponding to an F-16 in trimmed wings-level flight at 15,000 ft and 315 KTAS (532 ft/s) as given in Table 1 [Stevens and Lewis(1992)]. The value for Q_V was selected such that the rendezvous is completed with minimal distance error, whereas some speed error is permissible. Results are shown in Figures 2 and 3. The numerical results shown in the figures conform to the statements made above regarding the condition $\mu \to \infty$. It can be seen that a conjugate point exists for $\mu < 0.015$.

A similar analysis was performed for the interception problem with $Q_V = 0$, and $a_e^{max} = 2$ ft/s^2. It was found that in this case a conjugate point exists only for $\mu < 1 \cdot 10^{-5}$.

Table 1 Parameter values for F-16 longitudinal dynamics model using ft-sec-rad units

M_α	-1.773	Y_β	-114.5	L_β	-24.69	N_β	6.771	τ_δ	0.0495
M_q	-0.932	Y_p	35.17	L_p	-2.416	N_p	-0.035	δ_{ele}^{max}	$25\frac{\pi}{180}$
$M_{\delta_{ele}}$	-7.381	Y_r	-1060	L_r	0.537	N_r	-0.334	δ_{ail}^{max}	$21.5\frac{\pi}{180}$
Z_α	-362.2	$Y_{\delta_{ail}}$	5.614	$L_{\delta_{ail}}$	-29.77	$N_{\delta_{ail}}$	-1.604	δ_{rud}^{max}	$30\frac{\pi}{180}$
Z_q	-32.72	$Y_{\delta_{rud}}$	16.39	$L_{\delta_{rud}}$	3.896	$N_{\delta_{rud}}$	-3.036		
$Z_{\delta_{ele}}$	-43.95	θ_0	0.066	V_0	532	g	32.17		

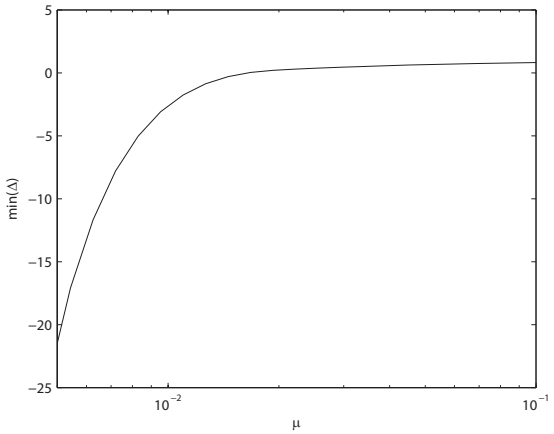

Fig. 2 Minimum Δ-values for $Q_V = 0.5$, $a_e^{max} = 2$ ft/s^2

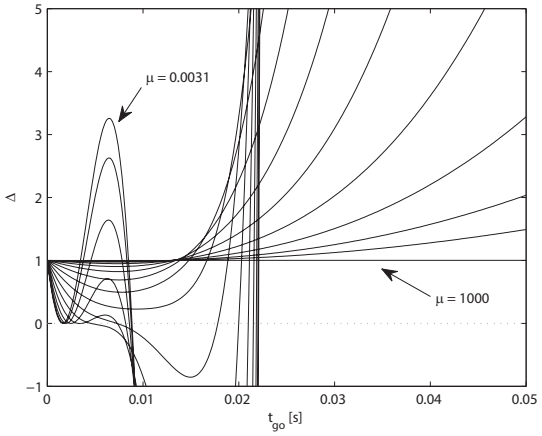

Fig. 3 Δ-values for $Q_V = 0.5$, $a_e^{max} = 2$ ft/s^2, $3.1 \cdot 10^{-3} \leq \mu \leq 1.0 \cdot 10^3$

3.4 Navigation Gains

By rewriting Eq. (34) the control law can be formulated as a function of the navigational gains $\mathbf{N}_{VZEM}$, $\mathbf{N}_{LZEM}$, $\mathbf{N}_{VZES}$, and $\mathbf{N}_{LZES}$ as

$$\mathbf{u}^*(t) = \frac{\mathbf{N}_{VZEM}}{\tau_\delta V_0} Z_1(t) + \frac{\mathbf{N}_{LZEM}}{\tau_\delta V_0} Z_2(t) + \frac{\mathbf{N}_{VZES}}{V_0} Z_3(t) + \frac{\mathbf{N}_{LZES}}{V_0} Z_4(t) \quad (46)$$

where the navigational gains are defined by (time indices are omitted for brevity)

$$\mathbf{N}_{VZEM} = V_0 \begin{bmatrix} \delta_{ele}^{max} \frac{\phi_{1,11} - \phi_{1,11}\kappa_2 + Q_V \kappa_4 \phi_{3,11}}{\alpha_1(\kappa_1 + \kappa_2 - \kappa_1\kappa_2 + \kappa_3\kappa_4 - 1)} \\ \mathbf{0}_{2\times 1} \end{bmatrix} \quad (47)$$

$$\mathbf{N}_{LZEM} = V_0 \begin{bmatrix} 0 \\ \delta_{ail}^{max} \frac{\phi_{2,12} - \phi_{2,12}\kappa_6 + Q_V \kappa_8 \phi_{4,12}}{\alpha_2(\kappa_5 + \kappa_6 - \kappa_5\kappa_6 + \kappa_7\kappa_8 - 1)} \\ \delta_{rud}^{max} \frac{\phi_{2,13} - \phi_{2,13}\kappa_6 + Q_V \kappa_8 \phi_{4,13}}{\alpha_3(\kappa_5 + \kappa_6 - \kappa_5\kappa_6 + \kappa_7\kappa_8 - 1)} \end{bmatrix} \quad (48)$$

$$\mathbf{N}_{VZES} = V_0 \begin{bmatrix} \delta_{ele}^{max} \frac{Q_V \phi_{3,11} + \phi_{1,11}\kappa_3 - Q_V \kappa_1 \phi_{3,11}}{\alpha_1 \tau_\delta(\kappa_1 + \kappa_2 - \kappa_1\kappa_2 + \kappa_3\kappa_4 - 1)} \\ \mathbf{0}_{2\times 1} \end{bmatrix} \quad (49)$$

$$\mathbf{N}_{LZES} = V_0 \begin{bmatrix} 0 \\ \delta_{ail}^{max} \frac{Q_V \phi_{4,12} + \phi_{2,12}\kappa_7 - Q_V \kappa_5 \phi_{4,12}}{\alpha_2 \tau_\delta(\kappa_5 + \kappa_6 - \kappa_5\kappa_6 + \kappa_7\kappa_8 - 1)} \\ \delta_{rud}^{max} \frac{Q_V \phi_{3,13} + \phi_{2,13}\kappa_7 - Q_V \kappa_5 \phi_{4,13}}{\alpha_3 \tau_\delta(\kappa_5 + \kappa_6 - \kappa_5\kappa_6 + \kappa_7\kappa_8 - 1)} \end{bmatrix} \quad (50)$$

The control input $\mathbf{u}^*$ is linear in the zero-effort vector and is bounded if all navigational gains are bounded, which is the case if and only if no conjugate

point exists. The denominator of every non-zero element in the navigational gain matrices contains one of the factors of Δ as defined in Eq. (37). Since $\Delta = 0$ at a conjugate point the navigational gains will become unbounded at such a point. In case a conjugate point exists the unbounded navigational gains will asymptotically approach $\pm\infty$ at the conjugate point and change sign if the sign of Δ changes.

Sign changes due to the non-minimum phase dynamics of the aircraft with regard to elevator control can be observed for all of the elements of the transition matrix that appear directly in the gains in Eq. (47) - Eq. (50). The sign changes occur at the point where the contribution by direct lift due to control surface deflection becomes larger than the contribution of the resulting angle of attack or side-slip angle. This point occurs at small values for t_{go} where the value of κ_i with $i \in \{1, 2, ..., 8\}$ is approaching zero. Hence the nominators of the navigational gains are dominated by the terms that are not multiplied by these values. Consequently, the navigational gains exhibit a change in sign at approximately the same time as the element of the transition matrix that occurs in the first term of their nominator.

If Q_V is set to zero (the interception problem), $\mathbf{N}_{VZES}$ and $\mathbf{N}_{LZES}$ are equal to zero for all t_{go}.

3.5 Optimal Trajectories

If Q_V, $\boldsymbol{\alpha}$, and $\boldsymbol{\beta}$ are set such that no conjugate point exists, then optimal trajectories can be calculated by integration of Eq. (19) with $\mathbf{u}(t) = \mathbf{u}^*(t)$ and $\mathbf{v}(t) = \mathbf{v}^*(t)$ as defined in Eq. (34) and Eq. (35), as long as $|u_i^*(t)| \leq 1 \; \forall t$ for $i \in \{1, 2, 3\}$ and $|v_i^*(t)| \leq 1 \; \forall t$ for $i \in \{1, 2\}$. Since $\dot{\mathbf{Z}}(t)$ is a linear function of $u(t)$ and $v(t)$, and $u^*(t)$ and $v^*(t)$ are both linear functions of $\mathbf{Z}(t)$; $\dot{\mathbf{Z}}(t)$ is also a linear function of $\mathbf{Z}(t)$. Consequently, any optimal trajectory $\mathbf{Z}(t)$ obtained using some Q_V, $\boldsymbol{\alpha}$, and $\boldsymbol{\beta}$ forms a linearly dependent set with any other optimal trajectory that is obtained using the same Q_V, $\boldsymbol{\alpha}$, and $\boldsymbol{\beta}$, if their initial conditions $\mathbf{Z}(0)$ are linearly dependent, no conjugate point exists, and the control saturation constraints are not violated.

Due to the fact that a linearized aircraft model is used, the pursuer's maximum acceleration is very large. If a negative unit step input is given to the elevator, an equilibrium for the vertical acceleration $\dot{V}_{p_h}$ is obtained at $\dot{V}_{p_h} \approx 500$ ft/s^2. However, in practice the maximum acceleration is never obtained by a control law based on a cost function with well tuned weights, due to the inclusion of $u(t)$ in Eq. (13).

Despite its larger maximum acceleration, the pursuer cannot guarantee a zero miss vector. This is due to the fact that the pursuer has second order dynamics, whereas the evader has ideal dynamics and thus can instantly apply an acceleration. As t_{go} nears zero the evader applies a large control action. Due to its higher order dynamics the pursuer is incapable of immediately

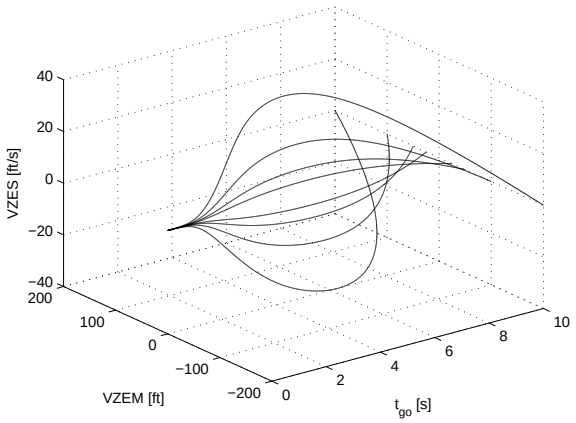

Fig. 4 Vertical optimal trajectories for $Q_V = 0.5$, $(\alpha_1, \alpha_2, \alpha_3) = (1, 2, 1)$, $(\beta_1, \beta_2) = (0.75, 0.75)$, and $a_e^{max} = 5$ ft/s^2

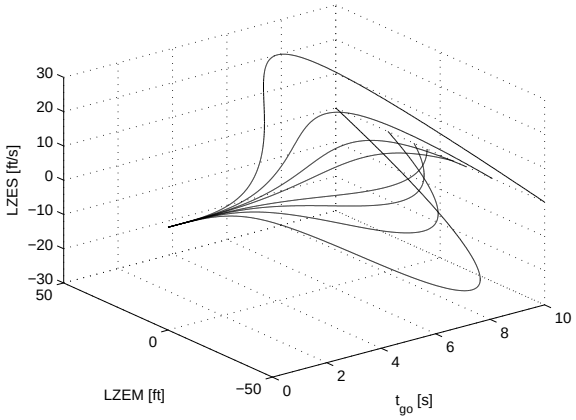

Fig. 5 Lateral optimal trajectories for $Q_V = 0.5$, $(\alpha_1, \alpha_2, \alpha_3) = (1, 2, 1)$, $(\beta_1, \beta_2) = (0.75, 0.75)$, and $a_e^{max} = 5$ ft/s^2

responding to the evader acceleration, resulting in an increase in miss distance and miss speed.

Figures 4 and 5 show optimal trajectories for $Q_V = 0.5$, $(\alpha_1, \alpha_2, \alpha_3) = (1, 2, 1)$, $(\beta_1, \beta_2) = (0.75, 0.75)$, and $a_e^{max} = 5$ ft/s^2. Again Q_V is selected such that rendezvous is achieved with minimum miss distance, while some speed difference is acceptable. The weight on aileron control action is increased in order to keep the roll angle within reasonable limits. Finally, $\boldsymbol{\beta}$ and a_e^{max} are chosen such that no conjugate point occurs, so that the obtained trajectory is optimal.

It should be noted that the vertical optimal trajectories in Figure 4 cannot be directly related to the lateral optimal trajectories in Figure 5. Due to decoupling of longitudinal and lateral-directional dynamics, there is no longitudinal control action due to lateral-directional states and vice versa. This is evidenced by the zero-valued elements of the navigation gains, Eq. (47) - Eq. (50), and results in uncoupled vertical and lateral optimal trajectories.

4 Simulation Results

In order to assess the performance of the guidance law two types of simulations were performed: The first type involves the LQ differential game guidance laws for both evader and pursuer, whereas the second type involves a burst noise signal as evader control.

4.1 Optimal Evader Guidance

Figures 6 and 7 show trajectory simulations corresponding to Figures 4 and 5. The simulation is initialized with the drogue located 100 ft above and 25 ft to the right of the pursuer aircraft. In order to prevent the occurrence of a conjugate point, the control weights $\boldsymbol{\alpha}$ and $\boldsymbol{\beta}$ cannot be decreased indefinitely, as described in Section 3.3. This causes both the evader and pursuer control inputs to remain small. The pursuer is however able to achieve small miss distance and speed. The terminal vertical and lateral distance are respectively 0.22 ft and -0.0093 ft, and the terminal vertical and lateral speed are 0.13 ft/s and 0.17 ft/s. The same values can also be found at $t_{go} = 0$ on the lines corresponding to $VZEM(t_{go} = 10) = -100$ ft in Figure 4 and $LZEM(t_{go} = 10) = -25$ ft in Figure 5. Vertical and lateral distance are reduced smoothly, while the angle of attack, sideslip angle, roll angle, and rotation rates remain well within operational limits.

4.2 Random Evader Guidance

For the simulation using burst noise evader control to mimic accelerations due to atmospheric turbulence, the evader control signal is divided into blocks of 0.4 s. Each block consists of a Gaussian white noise signal with $\sigma = 0.15$ and μ randomly selected to be either -0.5 or 0.5 separately for vertical and lateral acceleration.

An example of a simulation run using $Q_V = 0.5$, $(\alpha_1, \alpha_2, \alpha_3) = (1, 2, 1)$, $(\beta_1, \beta_2) = (0.75, 0.75)$, and $a_e^{max} = 5$ ft/s^2 and starting at -100 ft vertical

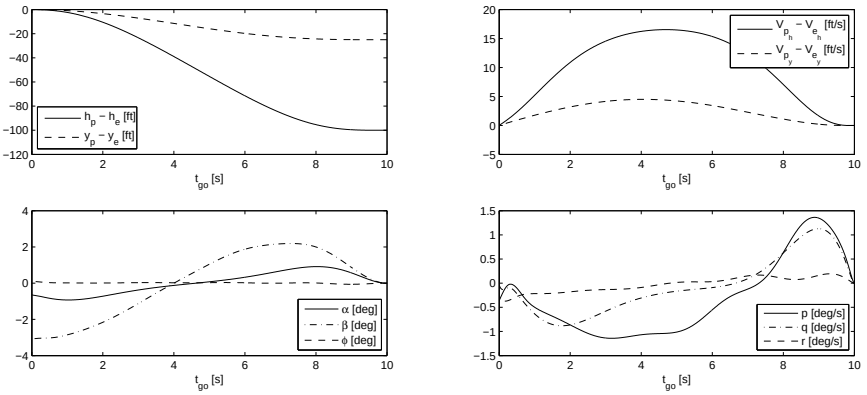

Fig. 6 Optimal evader and pursuer guidance trajectory for $Q_V = 0.5$, $(\alpha_1, \alpha_2, \alpha_3) = (1, 2, 1)$, $(\beta_1, \beta_2) = (0.75, 0.75)$, and $a_e^{max} = 5$ ft/s^2

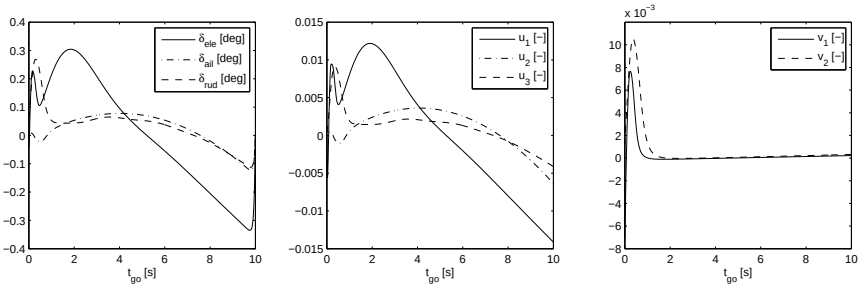

Fig. 7 Optimal evader control surface deflection and control inputs, and pursuer control inputs for $Q_V = 0.5$, $(\alpha_1, \alpha_2, \alpha_3) = (1, 2, 1)$, $(\beta_1, \beta_2) = (0.75, 0.75)$, and $a_e^{max} = 5$ ft/s^2

distance and -25 ft lateral distance is shown in Figures 8 and 9. It can clearly be seen that the evader control action is much larger than for the optimal evasion guidance. Consequently, a larger control action is also applied by the pursuer. The condition $|u_i| \leq 1$ for $i \in \{1, 2, 3\}$ is still satisfied though.

Larger angle of attack, sideslip angle, and roll angle are reached, due to the increase in control action. Also the roll rate reaches rather large values, but does reduce during the final part of the trajectory. However, for runs in which the evader control had several successive blocks with equal μ values towards the end of the trajectory larger terminal rotation rates and roll angles were observed.

A 10,000 run Monte Carlo simulation was performed using the burst noise evader control signal and $Q_V = 0.5$, $(\alpha_1, \alpha_2, \alpha_3) = (1, 2, 1)$, $(\beta_1, \beta_2) = (0.75, 0.75)$, and $a_e^{max} = 5$ ft/s^2. Accumulated terminal total distance and total relative speed are shown in Figure 10. These values are defined by the

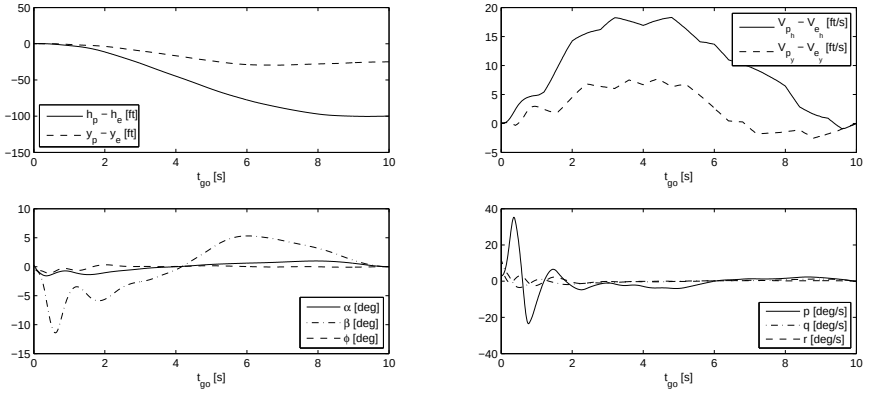

Fig. 8 Random evader and optimal pursuer guidance trajectory for $Q_V = 0.5$, $(\alpha_1, \alpha_2, \alpha_3) = (1, 2, 1)$, $(\beta_1, \beta_2) = (0.75, 0.75)$, and $a_e^{max} = 5$ ft/s^2

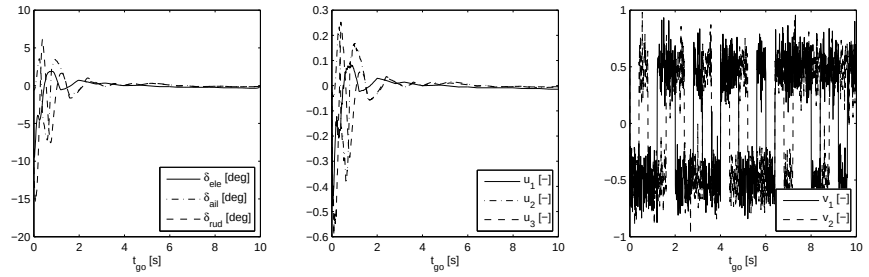

Fig. 9 Random evader control surface deflection and control inputs, and pursuer control inputs for $Q_V = 0.5$, $(\alpha_1, \alpha_2, \alpha_3) = (1, 2, 1)$, $(\beta_1, \beta_2) = (0.75, 0.75)$, and $a_e^{max} = 5$ ft/s^2

Euclidean norm of their respective vertical and lateral components. In all of the runs the magnitude of the terminal distance is below 0.50 ft, and the magnitude of the terminal speed is below 0.30 ft/s. The mean terminal distance is 0.22 ft, and the mean terminal speed is 0.20 ft/s. The terminal distance and speed results are negatively correlated with a Kendall's τ value of -0.23 ($p < 1 \cdot 10^{-100}$).

5 Concluding Remarks

In this article LQ differential game-based guidance was presented to be a viable option for control of an aircraft during refueling rendezvous. The con-

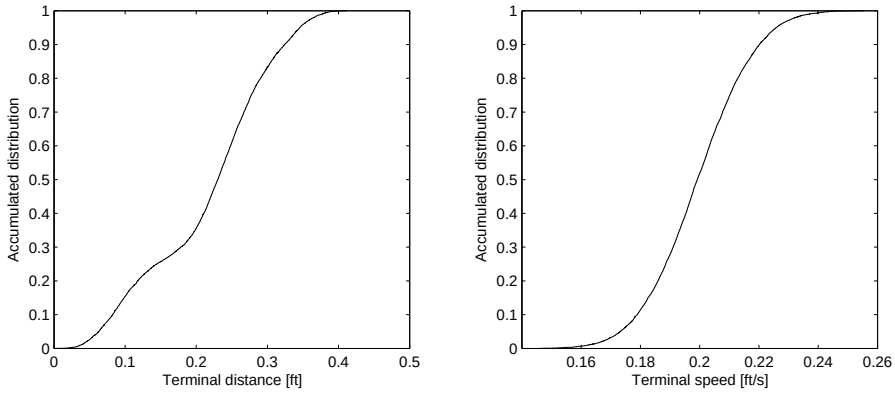

Fig. 10 Accumulated properties of Monte Carlo simulation results using $Q_V = 0.5$, $(\alpha_1, \alpha_2, \alpha_3) = (1, 2, 1)$, $(\beta_1, \beta_2) = (0.75, 0.75)$, and $a_e^{max} = 5$ ft/s^2, and burst noise evader control

trol method is capable of dealing with the complexity of the dynamics. It is however not able to guarantee zero miss for the rendezvous problem.

The results of a Monte Carlo simulation using burst noise evader control were presented. Results show promise, although there were issues with large aircraft rotations and rotation rates. Inclusion of these state variables in the cost function could potentially be a way to mitigate these issues.

This article showed an initial study along with practical results. A more elaborate dynamics model will result in more realistic results. A non-linear 6 degree of freedom flight dynamic model could be used to study the effects of longitudinal lateral-directional coupling. During this research the probe position was assumed to coincide with the aircraft center of gravity, thus neglecting the influence of aircraft rotation on the miss.

Further research into the movement of the drogue is also recommended. The application of realistic turbulence models and the addition of a coupling that simulates the effect of the wake of the drogue on the receiver aircraft are recommended for the purpose of obtaining more accurate simulation results.

Acknowledgements This research was partially supported by the German-Israeli Foundation for Scientific Research and Development.

References

[Anderson(1981)] Anderson G (1981) Comparison of optimal control and differential game intercept missile guidance laws. Journal of Guidance, Control, and Dynamics 4(2):190–115

[Bryson and Ho(1969)] Bryson A, Ho Y (1969) Applied Optimal Control. Blaisdell Publishing Company, New York

[Ochi and Kominami(2005)] Ochi Y, Kominami T (2005) Flight control for automatic aerial refueling via png and los angle control. In: AIAA Guidance, Navigation, and Control Conference and Exhibit

[Pachter et al.(1997)] Pachter M, Houpis C, Trosen D (1997) Design of an air-to-air automatic refueling flight control system using quantitative feedback theory. International Journal of Robust and Nonlinear Control 7:561–580

[Shima and Golan(2007)] Shima T, Golan O (2007) Linear quadratic differential games guidance law for dual controlled missiles. IEEE Transactions on Aerospace and Electronic Systems 43(3):834–842

[Shima et al.(2006)] Shima T, Idan M, Golan O (2006) Sliding-mode control for integrated missile autopilot guidance. Journal of Guidance, Control, and Dynamics 29(2):250–260

[Shinar and Shima(2012)] Shinar J, Shima T (2012) Differential game-based interceptor missile guidance. In: Balakrishnan S, Tsourdos A, White B (eds) Advances in Missile Guidance, Control, and Estimation, Automation and Control Series, CRC Press, Boca Raton, chap 9, pp 307–342

[Stevens and Lewis(1992)] Stevens B, Lewis F (1992) Aircraft Control and Simulation. Wiley Inter-Science, New York

[Tal and Shima(2015)] Tal E, Shima T (2015) Linear quadratic differential games guidance law for autonomous aerial refueling. In: Israel Annual Conference on Aerospace Sciences

[Tandale et al.(2006)] Tandale M, Bowers R, Valasek J (2006) Trajectory tracking controller for vision-based probe and drogue autonomous aerial refueling. Journal of Guidance, Control, and Dynamics 29(4):846–857

[Wang et al.(2008)] Wang J, Patel V, Cao C, Hovakimyan N, Lavretsky E (2008) Novel $\mathcal{L}_1$ adaptive control methodology for aerial refueling with guaranteed transient performance. Journal of Guidance, Control, and Dynamics 31(1):182–193